Analytical Methods

Accepted Manuscript

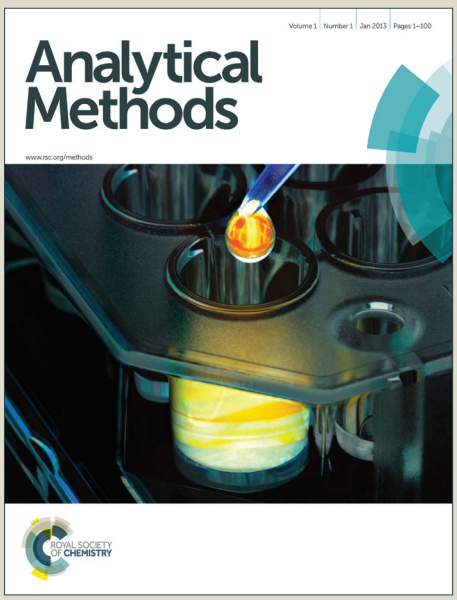

ROYAL SOCIETY OF CHEMISTRY

www.rsc.org/methods

Journal Name

RSCPublishing

ARTICLE

Simultaneous determination of hydroquinone and catechol using electrode modified by composite of graphene/lanthanum hydroxide nanowires

Cite this: DOI: 10.1039/x0xx00000x

Received 00th January 2012,
Accepted 00th January 2012

DOI: 10.1039/x0xx00000x

www.rsc.org/

Zhuo Guo*[a], Yin Lu[a], Jian Li*[b], Xian-feng Xu[a], Guo-qing Huang[a] and Ze-yu Wang[a]

A Nano-complex of Graphene and $La(OH)_3$ nanowires (GR-$La(OH)_3$) was prepared for the fabrication of voltammetric sensor used to simultaneously determine the two isomers of dihydroxybenzene, hydroquinone (HQ) and catechol (CC). The modified electrode exhibited excellent sensitivity and selectivity in determination of HQ and CC mixed in 0.1 M Na_2HPO_4-$C_4H_2O_7$ buffer solution (pH 4.0). Both HQ and CC could response to be a pair of quasi-reversible redox peaks and the potential difference between oxidation peaks of HQ and CC was 112 mv. Under the optimized condition, the oxidation peak current of both HQ and CC was linear over the range from 5 to 300 μM in the presence of 50 μM of the other one in the solution. The detection limit was found 0.015 μM for HQ and 0.01 μM for CC (S/N=3). The proposed method was further successfully applied to the simultaneous determination of HQ and CC in artificial wastewater samples, and the results showed good stability and high reproducibility.

Introduction

Hydroquinone (1,4-dihydroxybenzene, HQ) and catechol (1,2-dihydroxybenzene, CC) are environmental pollutants with high toxicity. The coexistence of the two dihydroxybenzene isomers leads to strong demand in developing analytical methods for simultaneous determination of HQ and CC with high sensitivity and selectivity. For this purpose, various methods including liquid chromatography,[1, 2] pH based flow injection analysis,[3] solid-phase extraction,[4] synchronous fluorescence,[5] spectrophotometry,[6, 7] gas chromatography-mass spectrometry[8] chemiluminescence[9] and electrochemical analysis[10-14] etc., have been established to achieve simultaneous determination of HQ and CC.

Among these above-mentioned methods, electrochemical analysis shows its unique advantages in fast response, cheap instrument, low cost, time saving, high sensitivity and excellent selectivity,[10-14] making it preferable and attractive for the simultaneous detection of the two isomers. Due to these advantages, many materials have been used to achieve sensitive and selective detection of HQ and CC, such as graphene,[15, 16] MWCNTs,[17, 18] conducting polymers,[19] MWCNTs+nanogold[20] composites film to improve their simultaneously detecting ability.

Graphene (GR) has been widely used in electronic, nanocomposites,[21-23] batteries,[24, 25] supercapacitors[26-28] and electrochemistry[29-32] areas due to its good electric conductivity, fast electron transfer rate, low cost and robust mechanical properties.[33, 34] Graphene based nano hybrids have shown potential applications in the area of chemical sensors, energy storage and catalysis.[35-37] The synergistic effect of such hybrids by dispersing nanostructured metal, metal oxide, metal hydroxide and metal sulfide on GR enhances their functionalities and thus exhibits excellent properties in a variety of applications.[38-43]

Among these inorganic compounds used in GR hybrids, nanostructured rare-earth materials have attracted lots of interest due to their unique chemical and physical properties originated from the electron transitions within the *4f* shell.[44, 45] These distinctive properties make rare earth materials suitable for applications in optical and magnetic fields, batteries, electrochemical sensor and catalysis supports.[46-48] Lanthanum hydroxide nanowires, as one of the important rare-earth compounds, have attracted attentions in electrochemical analysis area. Their nanostructured morphology has good film forming ability and can disperse those easily agglomerate components in complex.[49] The surface hydroxyl groups are able

to facilitate electronic transmission between electrode and analytes with hydrogen bonding groups.[50, 51]

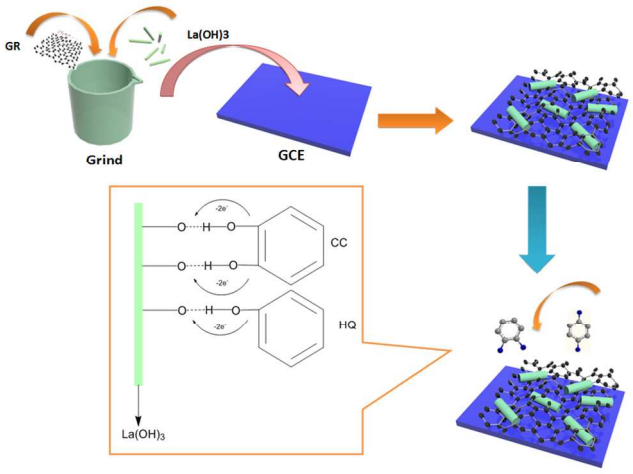

Figure 1. Schematic illustration of the fabrication process of electrochemical sensors for the determination of HQ and CC

Currently however, no report has been concerned using GR and $La(OH)_3$ nanorods hybrid to modify glass carbon electrode (GCE) on determination of HQ and CC. In this paper, we present an easy and general method to prepare a GR/$La(OH)_3$ hybrid material by a simple grinding method, using GR and $La(OH)_3$ nanowires as starting materials. Figure 1 illustrates the fabrication process of electrochemical sensor using GR and $La(OH)_3$ for the determination of HQ and CC. The GR/$La(OH)_3$ hybrid modified sensor exhibited sensitively simultaneous determination of HQ and CC due to its high surface area and enhanced catalytic activity, demonstrating great potential as an effective material in fabrication of electrochemical sensors.

Experimental

Reagents and instruments

Voltammetry including cyclic voltammetry (CV), differential pulse voltammetry (DPV) and electrochemical impedance spectroscopy (EIS) were performed on a Metrohm Autolab-PGSTAT302 electrochemical workstation. A three-electrode system was used with a GR-$La(OH)_3$/GCE as working electrode, a saturated calomel electrode (SCE) as reference electrode and a platinum wire as counter electrode. X-ray powder diffraction patterns were obtained on a Siemens D5005 X-ray powder diffraction apparatus using CuKα radiation (k = 0.15418 nm). Transmission electron micrographs (TEM) were obtained on a Hitachi 600 using a copper grid type sample holder.

Hydroquinone, catechol, La_2O_3 and other chemicals were analytical grade and were purchased from Aladdin Reagent Co. (Shanghai, China). Graphene was purchased from Nanjing Xianfeng Nano Co. (Nanjing， China). The water used was double-distilled. All the other chemicals were analytical grade and were used without further purification. Na_2HPO_4-$C_4H_2O_7$ buffer solution (0.1 M) with various pH values was used as supporting electrolyte. The stock solution (0.1 M) of HQ or CC was freshly prepared by dissolving HQ or CC in Na_2HPO_4-$C_4H_2O_7$ buffer solution (0.1 M, pH 4.0) using an ultrasonicator and stored at 4 ˚C. HQ and CC solutions with various concentrations were prepared by diluting the stock solution in buffer.

Preparation of nanosized lanthanum hydroxide ($La(OH)_3$)

The preparation of nanosized $La(OH)_3$ was adapted from the previous report.[52] In a typical synthesis, 0.5 g of La_2O_3 were dissolved in nitric acid (10%, 10 ml) to form an aqueous solution, then 10% KOH solution was added dropwise to adjust the pH 12-14. The as-obtained colloidal precipitate was transferred into a 50 ml autoclave, sealed and heated at 120 ˚C for 24 h. The autoclave was then allowed to cool to room temperature naturally. The precipitate was filtered, washed with water remove ions possibly remnant in the final products, and dried at 80 ˚C in air.

Preparation of GR-$La(OH)_3$

The hybrid was prepared by mixing GR with nanosized $La(OH)_3$ on a weight ratio of 1.5:1 in an agate mortar. The mixture was ground by hand for 1 h, producing a colloidal powder with uniform black-brown colour. The powder was readily dispersed in water by vigorous ultrasonication of the solution (1.0 mg mL^{-1}). The final solution was denoted as GR-$La(OH)_3$.

Preparation of the hydroquinone and catechol sensor

A glass carbon electrode (GCE) was firstly polished stepwise with 1.0, 0.3 and 0.05 μm alumina powders on silk, and then washed with ethanol/water (1:1, V/V) and double-distilled water in an ultrasonic bath for 30 min, separately. For preparing the hydroquinone and catechol sensor (denoted as GR-$La(OH)_3$/GCE), 10.0 μL of resulting GR-$La(OH)_3$ colloid was coated onto the surface of GCE and allowed to dry under an infrared lamp in the air. For comparison, GR/GCE and $La(OH)_3$/GCE were also fabricated using the same procedure. These electrodes were ready for measurement.

Results and discussion

Characterization of $La(OH)_3$ and GR-$La(OH)_3$

As shown in Figure 2, the reflection patterns of the hydrothermal products can be readily indexed to that of the hexagonal phase (space group $P6_3/m$) of $La(OH)_3$ with lattice constants a=6.5470 and c=3.8545 Å (JCPDS 83-2034).[52] XRD characterization indicated the successful synthesis of $La(OH)_3$, and the broaden peaks showed nanosized scale of products.[50]

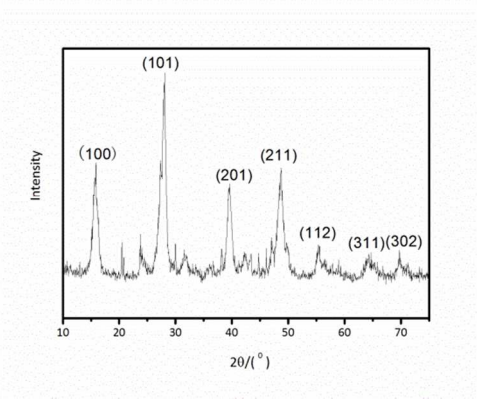

Figure 2. X-ray powder diffraction pattern of $La(OH)_3$.

Further characterization of size and morphology of GR-$La(OH)_3$ complex was confirmed by TEM. Figure 3 clearly illustrates $La(OH)_3$ nanorods are supported and well distributed on the surface of GR. Most of the $La(OH)_3$ products show nanorod morphologies with diameters of 10-20 nm and lengths of up to 150 nm.

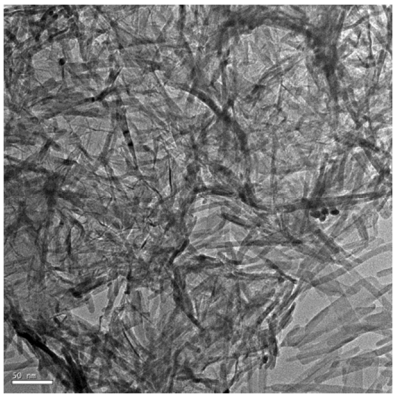

Figure 3. TEM image of the GR-La(OH)3 nanowires complex

Electrochemical characterization of modified electrodes

These modified electrodes were first characterized by comparing electrochemical behaviours of $K_3[Fe(CN)_6]$ at each electrode. Figure 4A showed the CVs recorded using these modified electrodes in the mixture solution of 1.0 mmol/L $K_3[Fe(CN)_6]$ and 0.5 mol/L KCl. On the bare GCE (curve a), a pair of well-defined redox peaks appeared with the lowest redox peak currents among all the electrodes, and the peak-to-peak separation (ΔE_p) was calculated as 0.403 V. At the $La(OH)_3$/GCE (curve b), the redox peak currents increased while the ΔE_p value decreased to 0.351 V, which indicated that the electron transfer of ferricyanide on GCE was enhanced by the modification of using $La(OH)_3$. This result can be attributed to the presence of nanosized $La(OH)_3$ on the electrode surface, which improved the reversibility of electrode reaction.

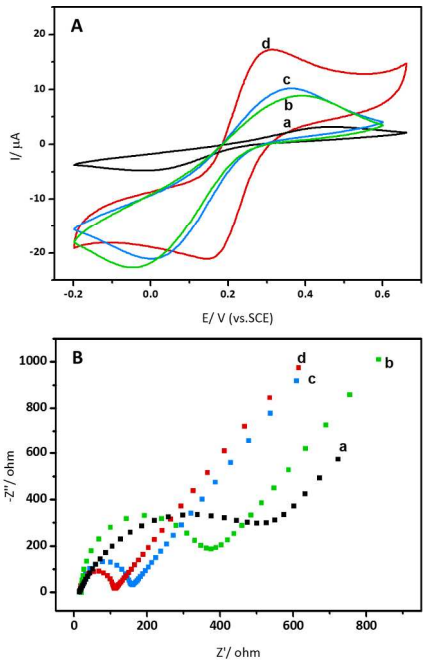

Figure 4. (A) CVs of bare GCE (a), $La(OH)_3$/GCE (b), GR/GCE (c), and GR-$La(OH)_3$/GCE (d) in 1.0 mmol/L $[Fe(CN)_6]^{3-/4-}$ solution containing 0.5 mol/l KCl. (B) Electrochemical impedance spectra of bare GCE (a), $La(OH)_3$/GCE (b), GR/GCE (c), and GR- $La(OH)_3$/GCE (d) in 1.0 mmol/L $[Fe(CN)_6]^{3-/4-}$ solution containing 0.5 mol/l KCl..

At the GR/GCE (curve c), the redox peak currents also increased with the ΔE_p of 0.304 V, which could be attributed to the excellent electric conductivity and fast electron transfer rate of GR film on the electrode surface. The highest redox peak currents appeared at the GR-$La(OH)_3$/GCE (curve d), with the lowest ΔE_p value of 0.142 V. The results could be attributed to the synergistic effect of GR-$La(OH)_3$ composite, which enhanced the whole interfacial conductivity by increasing the effective area on the electrode surface.[53]

Electrochemical impedance spectroscopy (EIS) is a powerful tool for studying the capability of electron transfer on the surface of different electrodes. Figure 4B illustrated the typical results of EIS of the bare GCE, $La(OH)_3$/GCE, GR/GCE and GR-$La(OH)_3$/GCE, respectively. Obviously, the whole profile for bare GCE exhibited the largest semicircle, showing the lowest electron transfer rate. The curve of $La(OH)_3$/GCE, GR/GCE and GR-$La(OH)_3$/GCE exhibited gradually smaller radius of semicircles compared with bare GCE, which showed that the presence of $La(OH)_3$ and GR could effectively accelerate the electron transfer. And the smallest radius of GR-$La(OH)_3$/GCE showed that their complex are able to synergistically accelerate the electron transfer on the electrode surface.

Cyclic voltammetric behaviour of modified electrodes

The electrochemical behaviours of HQ and CC at the bare GCE, $La(OH)_3$/GCE, GR/GCE and GR-$La(OH)_3$/GCE in 0.1 M Na_2HPO_4-$C_4H_2O_7$ buffer solution (pH 4.0) were studied using CV (Figure 5). In Figure 5A, a pair of weak redox peaks for HQ was observed on the bare GCE (curve a). When using

$La(OH)_3$/GCE as electrode, the redox peaks became relatively stronger (curve b). The anodic and cathodic peaks of HQ were observed at 381 and 16 mv and ΔE_p was calculated as 365 mv. While at the GR/GCE (curve c), the intensity of anodic and cathodic peaks increased, and the anodic and cathodic peaks appeared at 371 and 133 mv, respectively, which indicated that modification of GR effectively increased surface area of the electrode. At the GR-$La(OH)_3$/GCE (curve d), the intensity of both anodic and cathodic peaks greatly increased. The anodic and cathodic peaks were observed at 239 and 194 mv, respectively. Apart from the increased peak intensity, the anodic peak potential shifted from 381 mv to 239 mv and the cathodic peak potential shifted positively from 16 mv to 194 mv, leading to a dramatically reduced ΔE_p of only 45 mv, which can be attributed to the synergistic effect of GR-$La(OH)_3$ on GCE. These results demonstrated that the overpotential of HQ at GR-$La(OH)_3$/GCE has been remarkably lowered and the electrochemical reversibility of HQ at GR-$La(OH)_3$/GCE has been strongly improved, indicating the modification of GCE using GR-$La(OH)_3$ can significantly accelerate the electron transfer.

The electrochemical behaviour of CC at these different electrodes was also studied under the same condition and the CVs were shown in Figure 5B. There is no redox peak for CC at the bare GCE (curve a'). Redox peaks of CC were shown at all the other modified electrodes, and ΔE_p of CC at each modified electrode was gradually reduced in a sequence of $La(OH)_3$/GCE (curve b'), GR/GCE (curve c') and GR-$La(OH)_3$/GCE (curve d'). In addition, the anodic peak current also greatly increased at the same order. The above results further confirmed that the overpotential of CC at GR-$La(OH)_3$/GCE can be significantly lowered and the electrochemical reversibility of CC at the GR-$La(OH)_3$/GCE can be greatly improved, similar to the observation in the case of HQ at the GR-$La(OH)_3$/GCE. The experimental conditions were further optimized and described in the Supplementary Information.

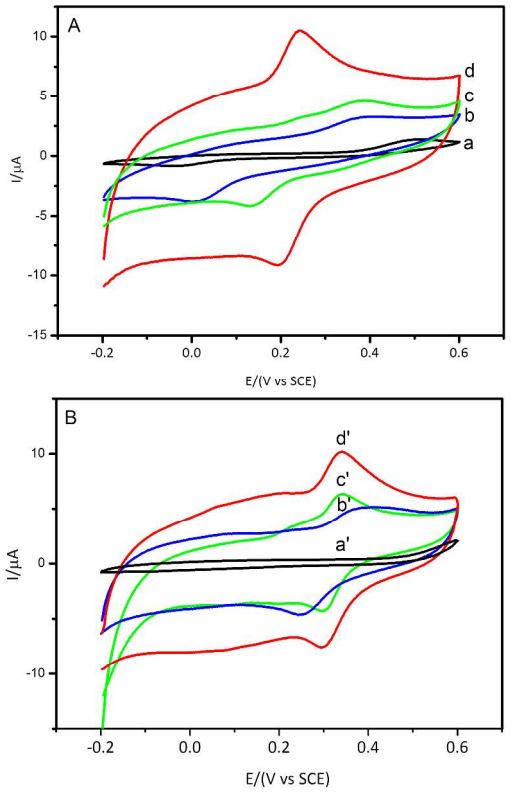

Figure 5. Cyclic voltammograms of 1.0×10^{-5} M HQ (A) and 1.0×10^{-5} M CC (B) in pH 4.0 Na_2HPO_4-$C_4H_2O_7$ buffer solution at bare GCE(a, a'), $La(OH)_3$/GCE (b, b'), GR/GCE (c, c') and GR-$La(OH)_3$/GCE(d, d').

Individual determination of HQ and CC

DPV was employed for simultaneous determination of HQ and CC at the GR-$La(OH)_3$/GCE because of its higher current sensitivity and better resolution compared with CV. The individual determination of HQ or CC in their mixture was performed at the GR-$La(OH)_3$/GCE with changing the concentration of one species while fixing that of another. Figure 6A shows DPV curves of different concentrations of HQ in 0.1 M buffer solution (pH 4.0) with the presence of a fixed concentration of CC (1.0×10^{-5} M). With the increase of concentration, the anodic peak currents of HQ were enhanced and were proportional to the concentration from 5.0×10^{-6} to 3.0×10^{-4} M. The linear regression equations can be expressed in the two concentration ranges as follows:

I_{pa}=18.60 + 0.138C (I_{pa}: μA, C: μM) (5-50 μM) (r=0.996) (1)

I_{pa}=21.97 + 0.052C (I_{pa}: μA, C: μM) (50-300 μM) (r=0.997) (2)

and the detection limit of HQ is 1.5×10^{-8} M with a signal-to-noise ratio (S/N) of 3. Similarly, as shown in Figure 6B, when keeping a constant concentration of HQ at 1.0×10^{-5} M, the anodic peak current of CC increased linearly to the concentration from 5.0×10^{-6} to 3.0×10^{-4} M. The linear equations in the two concentration ranges can be obtained as

I_{pa}=16.86 + 0.159C (I_{pa}: μA, C: μM) (5-30 μM) (r=0.997) (3)

I_{pa}=20.19 + 0.045C (I_{pa}: μA, C: μM) (30-300 μM) (r=0.997) (4)

and the detection limit is 1.0×10^{-8} M (S/N=3). All of the above results show that the proposed method has provided a sensitive determination of the two dihydroxybenzene isomers without interference from each other.

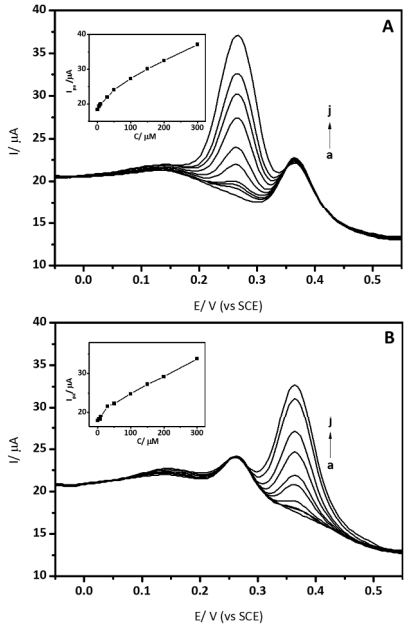

Figure 6. (A) DPV graphs of (a) 0 M, (b) 5×10^{-6} M, (c) 7.5×10^{-6} M, (d) 1.0×10^{-5} M (e) 3.0×10^{-5} M, (f) 5.0×10^{-5} M, (g) 1.0×10^{-4} M, (h) 1.5×10^{-4} M, (i) 2.0×10^{-4} M and (j) 3.0×10^{-4} M HQ in the presence of 5×10^{-5}M CC. Inset is the calibration plots of HQ. (B) DPV graphs of: (a) 0 M, (b) 5×10^{-6} M, (c) 7.5×10^{-6} M, (d) 1.0×10^{-5} M (e) 3.0×10^{-5} M, (f) 5.0×10^{-5} M, (g) 1.0×10^{-4} M, (h) 1.5×10^{-4} M, (i) 2.0×10^{-4} M and (j) 3.0×10^{-4} M CC in the presence of 5×10^{-5} M HQ. Inset is the calibration plots of CC.

Simultaneous determination of HQ and CC

Figure showed DPV curves collected by detecting HQ and CC in a mixture solution while their concentrations were simultaneously changed. Two well-defined oxidation peaks appeared and were independent on each other without interference. The simultaneous detection of HQ and CC on GR-La(OH)$_3$/GCE was therefore successfully achieved with a separation of their oxidation peak potentials at 112 mV. Meanwhile a comparison of the proposed method for determination of HQ and CC at other modified electrodes is listed in Table 1. It can be seen that the sensitivity of the proposed method is higher than or comparative to the other reported electrochemical methods.

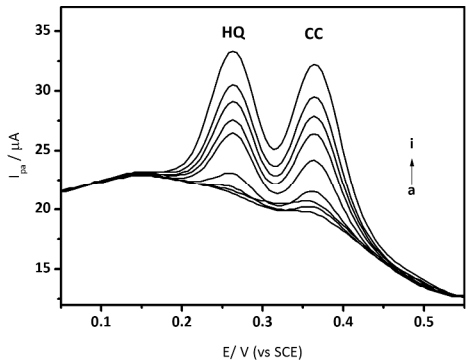

Figure 7. DPV of various concentrations of HQ and CC from a to i: (a) 5×10^{-6} M, (b) 7.5×10^{-6} M, (c) 1.0×10^{-5} M (d) 3.0×10^{-5} M, (e) 5.0×10^{-5} M, (f) 1.0×10^{-4} M, (g) 1.5×10^{-4} M, (h) 2.0×10^{-4} M and (i) 3.0×10^{-4} M.

Reproducibility and regeneration of the GR-La(OH)$_3$/GCE

The reproducibility of GR-La(OH)$_3$/GCE was examined by the detection of 5.0×10^{-5} M HQ in 0.1 M buffer solution (pH 4.0) for five successive determinations. The relative standard deviation (RSD) is 1.39%, showing that GR-La(OH)$_3$/GCE has good reproducibility. The fabrication reproducibility was also estimated with five different electrodes, which were fabricated independently by the same procedure. The RSD is 4.1 % for the peak current measuring in 5.0×10^{-5} M HQ, which demonstrates the reliability of the fabrication procedure. At the same time, the stability of one GR-La(OH)$_3$/GCE electrode was also investigated two weeks after fabrication. The current responded approximately 91.4% of the originally measured value. The excellent long-term stability and reproducibility of the composite electrode make them attractive in the fabrication of electrochemical sensors.

Effect of interfering substances

The influence of various substances on determination of 5.0×10^{-5} M HQ and CC was studied by DPV. It is found that 1000-fold Na^+, K^+, NH_4^+, Mg^{2+}, Ca^{2+}, Cu^{2+}, Zn^{2+}, Fe^{2+}, Cl^-, NO_3, SO_4^{2-}, L-cysteine, ascorbic acid, uric acid and phenol did not interfere with the DPV signals of targeting analytes at GR-La(OH)$_3$/GCE, indicating the proposed sensor has a high selectivity and good anti-interference ability. Figure showed the typical current-time response curves of GR-La(OH)$_3$/GCE to several materials.

Analytical applications

To investigate the applicability of the proposed method for simultaneous determination of HQ and CC, GR-La(OH)$_3$/GCE was applied in quantitative analysis of local tap water samples. Since the amounts of HQ and CC were unknown in tap water samples, the spike and recovery experiments were performed by measuring the DPV responses to the samples in which the known concentrations of HQ and CC were added. The amounts of HQ and CC in the tap water sample were determined by calibration method and were summarized in

Table **2**. The recoveries were 99.33-101.50% for HQ and 97.50-100.50% for CC, indicating the satisfactory applicability and reliability of the proposed method.

Table 1. Comparison of the fabricated electrode for HQ and CC detection with other electrodes.

Electrode	Method	Isomer	Linear range(μM)	Detection Limit(μM)	Ref.
GR-$La(OH)_3$/GCE	DPV	HQ	5-300	0.015	This work
		CC	5-300	0.010	
Go-MnO_2/GCE	DPV	HQ	0.01-0.07	0.007	[54]
		CC	0.03-1	0.01	
GR/GCE	DPV	HQ	1-50	0.015	[16]
		CC	1-50	0.01	
Pyridine-NG	DPV	HQ	5-200	0.38	[55]
		CC	5-200	1	
RGO-MWNTs/GCE	DPV	HQ	8.0-391.0	2.6	[56]
		CC	5.5-540.0	1.8	
PCV-GR/CILE	DPV	HQ	0.12-600	0.033	[53]
		CC	0.36-600.0	0.097	
GR-OMC/GCE	DPV	HQ	2-50	0.37	[57]
		CC	2-70	0.31	
MWNTs-IL-Gel/GCE	DPV	HQ	0.2-35	0.18	[11]
		CC	0.18-35	0.06	
PIL-MWCNTs/GCE	DPV	HQ	1–500	0.4	[10]
		CC	1-400	0.17	
CMK-3/GCE	DPV	HQ	10-200	0.076	[58]
		CC	10-300	0.1	
Carbon nanoparticle-chitosan composite	DPV	HQ	0.8-100	0.2	[59]
		CC	0.8-100	0.2	

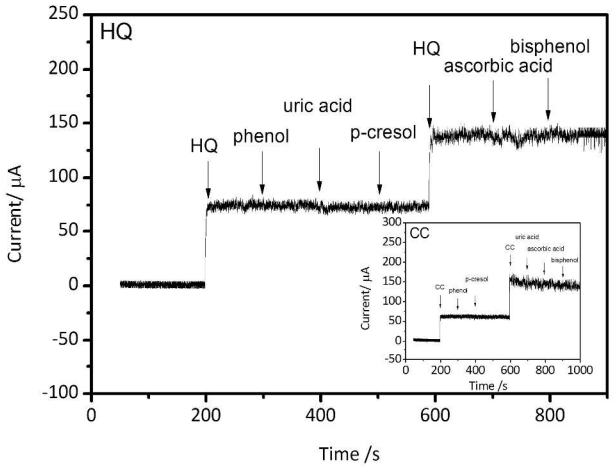

Figure 8. The amperometric response of 1.0×10^{-4} M phenol, uric acid, *p*-cresol, ascorbic acid at bisphenol at the GR-$La(OH)_3$/GCE spiked with 1.0×10^{-6} M HQ in stirred 0.1 M Na_2HPO_4-$C_4H_2O_7$ buffer solution. Applied potential: 0.24 V. Inset: the amperometric response of 1.0×10^{-4} M phenol, *p*-cresol, ascorbic acid, uric acid and bisphenol at the GR-$La(OH)_3$/GCE spiked with 1.0×10^{-6} M CC in stirred 0.1 M Na_2HPO_4-$C_4H_2O_7$ buffer solution. Applied potential: 0.35 V.

Table 2. Recovery results for HQ and CC in tap water.

Sample No.	Added (μM)		Found (μM)		Recovery (%)	
	HQ	CC	HQ	CC	HQ	CC
1	20	60	20.30	59.70	101.5	99.50
2	30	50	29.80	49.10	99.33	98.20
3	40	40	39.80	40.20	99.50	100.50
4	50	30	50.60	29.40	101.20	98.00
5	60	20	59.80	19.50	99.67	97.50

Conclusions

An electrochemical analysis method with high sensitivity and selectivity for simultaneous measurement of HQ and CC was developed by using GR-$La(OH)_3$ modified electrode, since GR-$La(OH)_3$ hybrids are able to facilitate electron transfer due to their excellent catalytic activity, high surface area and nanosized structure. Under the optimum condition, the modified electrode showed good selectivity, excellent linear relation from 5 to 300 μM and high sensitivity with a detection limit of 0.015 μM for HQ and 0.010 μM for CC from their mixture solution. Moreover, the result also indicates GR and $La(OH)_3$ composite has good synergistic effects with the potential applications in the area of electrochemical analysis.

Acknowledgements

The present work was supported by the Outstanding Young Scientist Foundation of the Education Department of Liaoning Province, China (LJQ2012033).

Notes

[a]Department of Materials Science and Engineering, Shenyang University of Chemical Technology, Shenyang 110142, China. Email: guozhuochina@syuct.edu.cn

[b]Department of Chemistry, University of Pittsburgh, Pittsburgh, PA 15260, USA. Email: lijianmail@gmail.com

References

1. A. Asan and I. Isildak, *J. Chromatogr. A*, 2003, **988**, 145-149.
2. H. Cui, C. He and G. Zhao, *J. Chromatogr. A*, 1999, **855**, 171-179.
3. J. A. Garcia-Mesa and R. Mateos, *J. Agric. Food. Chem.*, 2007, **55**, 3863-3868.
4. Á. Kovács, M. Mörtl and A. Kende, *Microchem. J.*, 2011, **99**, 125-131.
5. M. F. Pistonesi, M. S. Di Nezio, M. E. Centurión, M. E. Palomeque, A. G. Lista and B. S. Fernández Band, *Talanta*, 2006, **69**, 1265-1268.
6. A. Afkhami and H. A. Khatami, *J. Anal. Chem.*, 2001, **56**, 429-432.
7. P. Nagaraja, R. A. Vasantha and K. R. Sunitha, *Talanta*, 2001, **55**, 1039-1046.
8. S. C. Moldoveanu and M. Kiser, *J. Chromatogr. A*, 2007, **1141**, 90-97.
9. S. Li, X. Li, J. Xu and X. Wei, *Talanta*, 2008, **75**, 32-37.
10. X. Feng, W. Gao, S. Zhou, H. Shi, H. Huang and W. Song, *Anal. Chim. Acta*, 2013, **805**, 36-44.

11. C. Bu, X. Liu, Y. Zhang, L. Li, X. Zhou and X. Lu, *Colloids Surf., B*, 2011, **88**, 292-296.
12. X. Yue, S. Pang, P. Han, C. Zhang, J. Wang and L. Zhang, *Electrochem. Commun.*, 2013, **34**, 356-359.
13. H. Yin, Q. Zhang, Y. Zhou, Q. Ma, T. liu, L. Zhu and S. Ai, *Electrochim. Acta*, 2011, **56**, 2748-2753.
14. K. He, X. Wang, X. Meng, H. Zheng and S.-i. Suye, *Sens. Actuators, B*, 2014, **193**, 212-219.
15. L. Wang, Y. Meng, Q. Chen, J. Deng, Y. Zhang, H. Li and S. Yao, *Electrochim. Acta*, 2013, **92**, 216-225.
16. H. Du, J. Ye, J. Zhang, X. Huang and C. Yu, *J. Electroanal. Chem.*, 2011, **650**, 209-213.
17. Z. Wang, S. Li and Q. Lv, *Sens. Actuators, B*, 2007, **127**, 420-425.
18. S. Korkut, B. Keskinler and E. Erhan, *Talanta*, 2008, **76**, 1147-1152.
19. W. Si, W. Lei, Y. Zhang, M. Xia, F. Wang and Q. Hao, *Electrochim. Acta*, 2012, **85**, 295-301.
20. D.-W. Li, Y.-T. Li, W. Song and Y.-T. Long, *Anal. Methods*, 2010, **2**, 837-843.
21. X. Wu, Y. Chai, R. Yuan, X. Zhong and J. Zhang, *Electrochim. Acta*, 2014, **129**, 441-449.
22. A. Wang, X. Li, Y. Zhao, W. Wu, J. Chen and H. Meng, *Powder Technol.*, 2014, **261**, 42-48.
23. J. Qian, X. Yang, L. Jiang, C. Zhu, H. Mao and K. Wang, *Sens. Actuators, B*, 2014, **201**, 160-166.
24. W. Dai, L. Yu, Z. Li, J. Yan, L. Liu, J. Xi and X. Qiu, *Electrochim. Acta*, 2014, **132**, 200-207.
25. P. Goli, S. Legedza, A. Dhar, R. Salgado, J. Renteria and A. A. Balandin, *J. Power Sources*, 2014, **248**, 37-43.
26. I. Shakir, *Electrochim. Acta*, 2014, **129**, 396-400.
27. Y. Wimalasiri, R. Fan, X. S. Zhao and L. Zou, *Electrochim. Acta*, 2014, **134**, 127-135.
28. J. Yang and L. Zou, *Electrochim. Acta*, 2014, **130**, 791-799.
29. W. Sun, L. Cao, Y. Deng, S. Gong, F. Shi, G. Li and Z. Sun, *Anal. Chim. Acta*, 2013, **781**, 41-47.
30. M. Pumera, *Electrochem. Commun.*, 2013, **36**, 14-18.
31. M. Cui, B. Xu, C. Hu, H. B. Shao and L. Qu, *Electrochim. Acta*, 2013, **98**, 48-53.
32. Y. Wang, H. Li and J. Kong, *Sens. Actuators, B*, 2014, **193**, 708-714.
33. Z. Luo, Y. Lu, L. A. Somers and A. T. C. Johnson, *J. Am. Chem. Soc.*, 2009, **131**, 898-899.
34. L. Zhang, S. Diao, Y. Nie, K. Yan, N. Liu, B. Dai, Q. Xie, A. Reina, J. Kong and Z. Liu, *J. Am. Chem. Soc.*, 2011, **133**, 2706-2713.
35. S. Pakapongpan, J. P. Mensing, D. Phokharatkul, T. Lomas and A. Tuantranont, *Electrochim. Acta*, 2014, **133**, 294-301.
36. Y. Zhang, H. Shu, G. Chang, K. Ji, M. Oyama, X. Liu and Y. He, *Electrochim. Acta*, 2013, **109**, 570-576.
37. J. M. Kim, W. G. Hong, S. M. Lee, S. J. Chang, Y. Jun, B. H. Kim and H. J. Kim, *Int. J. Hydrogen Energy*, 2014, **39**, 3799-3804.
38. S. Wang, S. P. Jiang and X. Wang, *Electrochim. Acta*, 2011, **56**, 3338-3344.
39. D.-L. Zhou, J.-J. Feng, L.-Y. Cai, Q.-X. Fang, J.-R. Chen and A.-J. Wang, *Electrochim. Acta*, 2014, **115**, 103-108.
40. Q. Shi, G. Diao and S. Mu, *Electrochim. Acta*, 2014, **133**, 335-346.
41. T. E. M. Nancy and V. A. Kumary, *Electrochim. Acta*, 2014, **133**, 233-240.
42. Y. J. Yang, W. Li and X. Wu, *Electrochim. Acta*, 2014, **123**, 260-267.
43. X. Zhang, F. Xu, B. Zhao, X. Ji, Y. Yao, D. Wu, Z. Gao and K. Jiang, *Electrochim. Acta*, 2014, **133**, 615-622.
44. X. Wang and Y. Li, *Chem. Eur. J.*, 2003, **9**, 5627-5635.
45. A. Tsubouchi and T. C. Bruice, *J. Am. Chem. Soc.*, 1995, **117**, 7399-7411.
46. X.-S. An, Y.-J. Fan, D.-J. Chen, Q. Wang, Z.-Y. Zhou and S.-G. Sun, *Electrochim. Acta*, 2011, **56**, 8912-8918.
47. K. Hachiya and H. Ohashi, *Electrochim. Acta*, 2007, **53**, 7-10.
48. Q. Li, J. Lin, J. Wu, Z. Lan, Y. Wang, F. Peng and M. Huang, *Electrochim. Acta*, 2011, **56**, 4980-4984.
49. Y. Zhang, R. Yuan, Y. Chai, X. Zhong and H. Zhong, *Colloids Surf., B*, 2012, **100**, 185-189.
50. C. G. Hu, H. Liu, W. T. Dong, Y. Y. Zhang, G. Bao, C. S. Lao and Z. L. Wang, *Adv. Mater.*, 2007, **19**, 470-474.
51. X. Wang and Y. Li, *Angew. Chem. Int. Ed.*, 2002, **41**, 4790-4793.
52. X. Wang, X. M. Sun, D. Yu, B. S. Zou and Y. Li, *Adv. Mater.*, 2003, **15**, 1442-1445.
53. W. Sun, Y. Wang, Y. Lu, A. Hu, F. Shi and Z. Sun, *Sens. Actuators, B*, 2013, **188**, 564-570.
54. T. Gan, J. Sun, K. Huang, L. Song and Y. Li, *Sens. Actuators, B*, 2013, **177**, 412-418.
55. H.-L. Guo, S. Peng, J.-H. Xu, Y.-Q. Zhao and X. Kang, *Sens. Actuators, B*, 2014, **193**, 623-629.
56. F. Hu, S. Chen, C. Wang, R. Yuan, D. Yuan and C. Wang, *Anal. Chim. Acta*, 2012, **724**, 40-46.
57. X. Yuan, D. Yuan, F. Zeng, W. Zou, F. Tzorbatzoglou, P. Tsiakaras and Y. Wang, *Appl. Catal. B*, 2013, **129**, 367-374.
58. J. Yu, W. Du, F. Zhao and B. Zeng, *Electrochim. Acta*, 2009, **54**, 984-988.
59. M. Amiri, S. Ghaffari, A. Bezaatpour and F. Marken, *Sens. Actuators, B*, 2012, **162**, 194-200.

Table of contents entry:

An electrochemical sensor modified by $La(OH)_3$ nanorods and graphene hybrids for simultaneous detection of hydroquinone and catechol.